31st Annual International Conference of the IEEE EMBS
Minneapolis, Minnesota, USA, September 2-6, 2009

Periodic contrast-enhanced computed tomography for thermal ablation monitoring: A feasibility study

Christopher L. Brace, *Member, IEEE; Charles A. Mistretta; J. Louis Hinshaw; Fred T. Lee, Jr.*

***Abstract*—Image-guided tumor ablation is rapidly gaining acceptance for treating many tumors. While imaging diagnosis, treatment targeting and follow-up continue to improve, little progress has been made in developing practical imaging techniques for monitoring ablation treatments. In this study we demonstrate the feasibility of using contrast-enhanced computed tomography (CECT) to monitor ablation zone growth with 2 min temporal resolution. Highly constrained back-projection (HYPR) post-processing is applied to the time-series of CECT images, improving image quality by a factor of four after acquiring ten time frames. Such improvements limit the amount of radiation and iodinated contrast material required to visualize the ablation zone, especially at early time points. Additional study of periodic CECT with HYPR processing appears warranted.**

I. Introduction

Image-guided, percutaneous thermal tumor ablation using radiofrequency (RF), laser or microwave energy is rapidly gaining acceptance as a treatment option for many tumors in the liver, lung, kidney and bones, with other areas under investigation [1-7]. Tumor ablation requires imaging for all aspects of the treatment: tumor diagnosis, localization and targeting, applicator guidance, treatment monitoring and imaging follow-up to assess procedural success. While advances in imaging technologies have improved all of these areas, very little progress has been made to improve practical intra-procedural treatment monitoring.

Current monitoring options include interstitial temperature probes, ultrasound imaging, and MRI. Interstitial temperature probes provide fast and accurate data, but very poor spatial resolution so are typically only used to prevent complications or ensure adequate coverage of a specific point [8]. Ultrasound imaging can also provide realtime feedback about treatment progress, but is obscured by bubbles created during high-temperature thermal ablation and can be used only to approximate the ablation zone geometry [9-10]. New reconstruction techniques may alleviate some of these problems, but are not yet widely available or clinically validated [11-13]. Finally, MRI temperature mapping provides fair spatial and temporal resolution, but few interventional MRI systems are available, scan-time is expensive, temperature imaging is relatively slow for volumetric data acquisition, and MRI-compatible ablation equipment is not widespread [14-15].

One alternative to ultrasound and MRI is computed tomography (CT). Contrast between ablated tissue and normal parenchyma is relatively low, so post-ablation imaging is typically performed using contrast-enhancement [16]. Contrast-enhanced (CE) scans are performed by injecting iodinated contrast material intravenously, then acquiring CT images when the contrast material reaches the target (eg, liver). Iodinated contrast causes signal enhancement, but cannot penetrate into coagulated ablation zones. Therefore, CECT can be used to improve visualization of ablation zones. However, CT uses ionizing radiation (x-rays) and repetitive scans using diagnostic radiation levels would potentially increase the risk of malignancies in the long-term [17].

Recently, an image processing technique known as HYPR has been described to increase the signal-to-noise ratio (SNR) in a series of images, while emphasizing changes that occur between images [18]. The boost in SNR allows lower radiation and contrast doses to be used, enabling the use of periodic CT for treatment monitoring.

Here we present a method for monitoring thermal ablations that uses periodic CECT with HYPR processing that does not increase accumulated radiation dose or contrast load beyond a typical diagnostic CECT. The goals of this preliminary study were to determine whether periodic CECT could be used to monitor treatment progress, and determine the benefit provided by HYPR imaging.

II. Methods

A. Ablation procedure

RF ablations were performed in vivo in the livers of three female domestic swine (wt = 50 kg). Prior to ablation, a roadmap CT scan was performed through the entire liver. A 3 cm, 17-gauge (1.5 mm diameter) water-cooled RF electrode was then placed percutaneously into the liver under CT guidance to avoid large vessels. Ablations were performed for 20 min using a maximum of 200 W with an impedance-based power pulsing algorithm (Valleylab Cool-tip, Boulder, CO). CECT images (80 kVp, 100 mA, 512x512, 1:1 helical pitch, 5 mm slice thickness) were acquired every 2 min during the ablation through a volume

Manuscript received April 23, 2009; revised June 16, 2009.

C. L. Brace is with the Departments of Radiology and Biomedical Engineering at the University of Wisconsin, Madison, WI 53705 USA (phone/fax: 608-262-4151; e-mail: clbrace@wisc.edu).

C. A. Mistretta is with the Department of Medical Physics at the University of Wisconsin, Madison, WI 53705 USA.

J. L. Hinshaw and F. T. Lee Jr. are with the Department of Radiology at the University of Wisconsin, Madison, WI 53792-3252 USA..

encompassing the entire ablation. The animal breath was held while imaging to reduce motion artifacts between imaging frames. A 15 ml bolus of contrast was injected (5 ml/s; Iohexol 300, GE Healthcare, Waukesha, WI) in 2 min intervals 30 s before each image acquisition to provide maximal uptake in the normal liver parenchyma. A 15 ml contrast dose was chosen so that the total contrast load would not exceed the normal maximum 150 ml (15 ml x 10 scans). CT imaging parameters were designed to limit accumulated radiation dose to that of a typical diagnostic scan. Accumulated radiation dose (CTDIvol) and contrast load were computed at each time point.

B. Image processing

After ablation, all CT data was downloaded to a separate workstation for processing. In each dataset, a single 2D slice from the center of the ablation, but without substantial streak artifact from the ablation electrode, was chosen for analysis. The same slice was used in each time frame to create the test image set for HYPR processing. Control images were left unprocessed. Test images were processed using the HYPR LR (local reconstruction) algorithm described previously but without needle registration or motion correction [19]. Briefly, a composite image was created by summing all of the slice images acquired up to and including the analysis time point. Input and composite images were blurred using a 5x5 unity convolution kernel, then divided to create the weighting image for each time frame. Finally, the HYPR image for each time frame was created by multiplying the composite by the weighting image (Figure 1). Images were processed using MATLAB 7.7.0 on a workstation with two 3.4 GHz Xeon processors and 4 GB of memory.

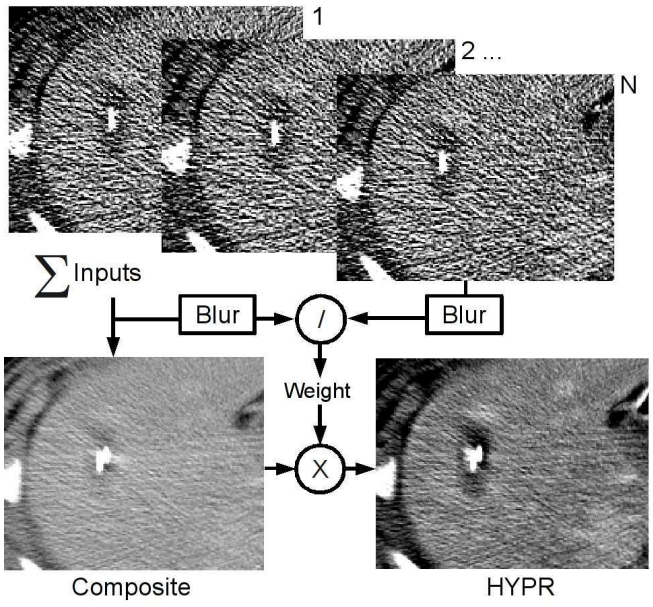

Figure 1: HYPR algorithm schematic.

C. Image quality comparisons

Image quality between control and HYPR images were compared in terms of overall signal-to-noise ratio (SNR) and contrast-to-noise ratio (CNR) between the ablation zone and normal liver background. Seven regions of interest, approximately 10 pixels in diameter – two inside the ablation zone and five in normal liver away from large vessels – were chosen for measurement. The same ROIs were used for all time frames. SNR in each tissue (ablated or normal) was defined as the ratio of mean pixel intensity (μ) to the standard deviation in pixel intensity (noise, σ) of the ROIs in that tissue:

$$SNR = \frac{\mu}{\sigma} \tag{1}$$

CNR was defined as the ratio of the difference in mean pixel intensity between normal and ablated ROIs to the standard deviation in pixel intensity in the normal tissue ROI:

$$CNR = \frac{\mu_{normal} - \mu_{ablated}}{\sigma_{normal}} \tag{2}$$

SNR and CNR measurements were calculated for each time frame in control and HYPR images. Mean SNR and CNR were calculated based on the three separate sets of data, one from each animal. SNR and CNR in control and HYPR images were compared using a t-tests at each time point with $P < .05$ indicating statistical significance.

III. Results

A. Periodic CT technique evaluation

All procedures were completed successfully without complication. CDTIvol was 2.5mGy per scan, for a total of 25 mGy, which is comparable to a typical diagnostic abdominal scan [20]. Total contrast load during each treatment was 150 ml.

The periodic CECT method was able to track ablation zone growth over time in 2 min intervals (Figure 2). Without post-processing, images were qualitatively noisy and difficult to interpret. Reading image data and HYPR processing an entire treatment took approximately 10 s of computational time. In HYPR-processed images, the ablation zone was clearly visible even after 4 min of heating, at which point accumulated radiation was 5.0 mGy and total contrast load was 30 ml. HYPR imaging improved the speed by which the ablation zone could be identified with periodic CECT.

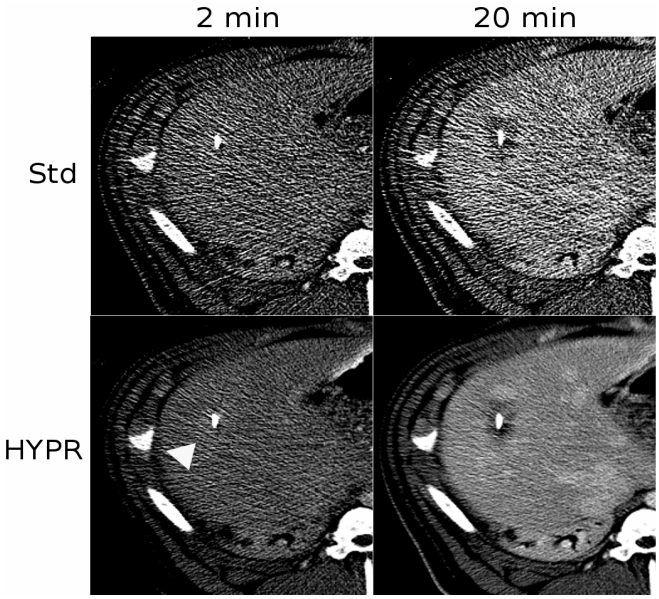

Figure 2: Image comparison of standard reconstruction versus HYPR post-processing after 2 and 12 min of heating. In this case, a slight contrast-enhancement was observed after 2 min of heating due to local blood flow increases (arrow). As the zone of coagulation grew, enhancement was replaced by a darker area of low-attenuation. Note that the HYPR-processed images contain less noise and more clearly define the ablation zone, which is darker than the enhancing liver. Blood vessels are clearly visible in the 20 min HYPR image but not in the standard image.

B. Image quality comparisons

HYPR processing was able to significantly increase SNR at each time point after 2 min over controls ($P < .05$, all comparisons), with a factor four improvement occurring after 20 min (Figure 2). SNR improvements increased over time, as more images were added to the composite for each time point and total contrast load increased as image noise decreased in HYPR images. Similarly, CNR was increased significantly at each time point after 2 min with HYPR processing ($P < .05$, all comparisons; Figure 4).

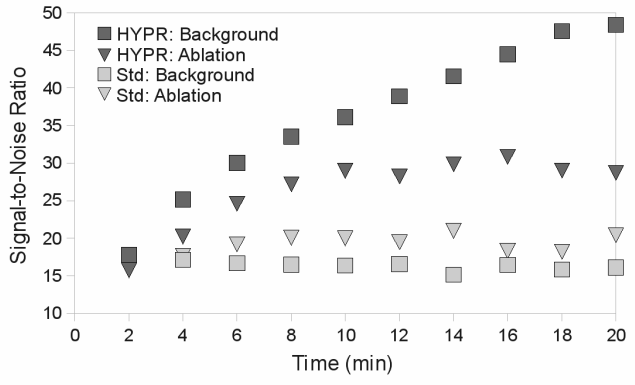

Figure 3: Mean ROI intensity versus time inside and outside of the ablation zone in images using standard reconstruction or HYPR post-processing. HYPR processing increased SNR by a factor of four over standard reconstruction after 20 min of heating.

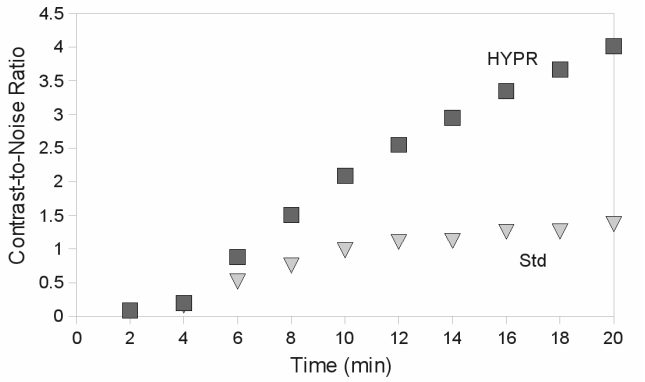

Figure 4: Mean CNR between ROIs in the ablation zone and in the background liver over time. The improvements in CNR with HYPR processing provide visualization of the ablation zone within 4-6 min, as compared to 12-14 min with standard reconstruction.

IV. Discussion

This study demonstrates the feasibility of using periodic CECT to observe ablation zone growth intra-procedurally. HYPR processing took only seconds to complete, implying that faster image acquisition is possible. HYPR was also able to improve image quality enough to keep accumulated radiation dose to normal diagnostic levels, and limit the amount of contrast material required for visualization of the ablation zone.

The ability to monitor ablation zone growth using CECT is of particular importance. Many image-guided interventions are guided and assessed using CT imaging, so physicians are already comfortable using the technology. CT suites are also widely available and usually more apt to be used for ablation procedures than MRI due to time and cost considerations. Thus, the ability to perform all functions of the ablation procedure (targeting, guiding, monitoring and verifying) with a common imaging modality makes this technique more accessible to more practitioners.

As a feasibility study, there were certain limitations to the implementation of both the periodic CECT method and HYPR processing. Additional studies are needed to identify the optimal combination of image acquisition rate, radiation dose per scan (ie, image quality per scan), contrast material injection rate and dose per injection. For example, the ablation zone appears to grow most rapidly in diameter during the first 5 min. Faster image acquisition during this time would improve monitoring. Smaller radiation doses may be possible with more images to add to the HYPR composite. Larger doses of contrast material at these earlier times may also improve visualization. Finally, optimized low-level code should help improve HYPR processing speed.

V. Conclusions

Periodic CECT is capable of monitoring ablation zone growth during RF ablation. HYPR processing facilitates the use of periodic CECT by improving image quality while limiting radiation dose and contrast load to acceptable levels.

Acknowledgment

The authors would like to thank Paul F. Laeseke, Lisa A. Sampson, Meghan Hanson and the radiation technology staff at the University of Wisconsin Hospitals and Clinics for their assistance with this study.

References

[1] R. Lencioni, D. Cioni, L. Crocetti, C. Franchini, C. D. Pina, J. Lera and C. Bartolozzi, "Early-stage hepatocellular carcinoma in patients with cirrhosis: long-term results of percutaneous image-guided radiofrequency ablation," *Radiology*, vol. 234, pp. 961-967, Mar. 2005.

[2] L. Solbiati, I. Tiziana, B. Michela and C. Luca, "Radiofrequency ablation of liver metastases of colorectal origin with intention to treat: local response rate and long-term survival over 7-year follow-up," presented at the Radiological Society of North America Annual Meeting, Chicago, IL, 2006.

[3] S. C. Rose, P. A. Thistlethwaite, P. E. Sewell and R. B. Vance, "Lung cancer and radiofrequency ablation," *J Vasc Interv Radiol*, vol. 17, pp. 927-951, Jun. 2006.

[4] R. J. Zagoria, M. A. Traver, D. M. Werle, M. Perini, S. Hayasaka and P. E. Clark, "Oncologic efficacy of ct-guided percutaneous radiofrequency ablation of renal cell carcinomas," *AJR Am J Roentgenol*, vol. 189, pp. 429-436, Aug. 2007.

[5] G. Manenti, F. Bolacchi, T. Perretta, E. Cossu, C. A. Pistolese, O. C. Buonomo, E. Bonanno, A. Orlandi and G. Simonetti, "Small breast cancers: in vivo percutaneous us-guided radiofrequency ablation with dedicated cool-tip radiofrequency system," *Radiology*, to be published.

[6] D. K. Bahn, P. Silverman, F. S. Lee, R. Badalament, E. D. Bahn and J. C. Rewcastle, "Focal prostate cryoablation: initial results show cancer control and potency preservation," *J. Endourol.*, vol. 20, pp. 688-692, Sep. 2006.

[7] J. M. Monchik, G. Donatini, J. Iannuccilli and D. E. Dupuy, "Radiofrequency ablation and percutaneous ethanol injection treatment for recurrent local and distant well-differentiated thyroid carcinoma," *Ann. Surg.*, vol. 244, pp. 296-304, Aug. 2006.

[8] R. I. Carey and R. J. Leveillee, "First prize: direct real-time temperature monitoring for laparoscopic and ct-guided radiofrequency ablation of renal tumors between 3 and 5 cm," *J. Endourol.*, vol. 21, pp. 807-813, Aug. 2007.

[9] J. R. Leyendecker, G. D. 3. Dodd, G. A. Halff, V. A. McCoy, D. H. Napier, L. G. Hubbard, K. N. Chintapalli, S. Chopra, W. K. Washburn, R. M. Esterl, F. G. Cigarroa, R. E. Kohlmeier and F. E. Sharkey, "Sonographically observed echogenic response during intraoperative radiofrequency ablation of cirrhotic livers: pathologic correlation," *AJR Am J Roentgenol*, vol. 178, pp. 1147-1151, May 2002.

[10] L. Solbiati, M. Tonolini and L. Cova, "Monitoring rf ablation," *Eur Radiol*, vol. 14 Suppl 8, p. P34-42, Oct. 2004.

[11] T. Varghese, U. Techavipoo, J. A. Zagzebski and F. T. J. Lee, "Impact of gas bubbles generated during interstitial ablation on elastographic depiction of in vitro thermal lesions," *J Ultrasound Med*, vol. 23, pp. 535-44, Apr. 2004.

[12] S. Bharat, T. G. Fisher, T. Varghese, T. J. Hall, J. Jiang, E. L. Madsen, J. A. Zagzebski and F. T. J. Lee, "Three-dimensional electrode displacement elastography using the siemens c7f2 foursight four-dimensional ultrasound transducer," *Ultrasound Med Biol*, vol. 34, pp. 1307-1316, Aug. 2008.

[13] J. Jiang, T. Varghese, C. Brace, E. Madsen, T. Hall, S. Bharat, M. Hobson, J. Zagzebski and F. Lee Jr, "Young's modulus reconstruction for radio-frequency ablation electrode-induced displacement fields: a feasibility study," *IEEE Trans Med Imaging*, to be published.

[14] B. D. de Senneville, C. Mougenot, B. Quesson, I. Dragonu, N. Grenier and C. T. W. Moonen, "Mr thermometry for monitoring tumor ablation," *Eur Radiol*, vol. 17, pp. 2401-2410, Sep. 2007.

[15] T. J. Vogl, N. N. N. Naguib, K. Eichler, T. Lehnert, H. Ackermann and M. G. Mack, "Volumetric evaluation of liver metastases after thermal ablation: long-term results following mr-guided laser-induced thermotherapy," *Radiology*, vol. 249, pp. 865-871, Dec. 2008.

[16] C. Schraml, S. Clasen, N. F. Schwenzer, I. Koenigsrainer, T. Herberts, C. D. Claussen and P. L. Pereira, "Diagnostic performance of contrast-enhanced computed tomography in the immediate assessment of radiofrequency ablation success in colorectal liver metastases," *Abdom Imaging*, vol. 33, pp. 643-651, Nov-Dec. 2008.

[17] E. J. Hall and D. J. Brenner, "Cancer risks from diagnostic radiology," *Br J Radiol*, vol. 81, pp. 362-378, May. 2008.

[18] C. A. Mistretta, O. Wieben, J. Velikina, W. Block, J. Perry, Y. Wu, K. Johnson and Y. Wu, "Highly constrained backprojection for time-resolved mri," *Magn Reson Med*, vol. 55, pp. 30-40, Jan. 2006.

[19] K. M. Johnson, J. Velikina, Y. Wu, S. Kecskemeti, O. Wieben and C. A. Mistretta, "Improved waveform fidelity using local hypr reconstruction (hypr lr)," *Magn Reson Med*, vol. 59, pp. 456-462, Mar. 2008.

[20] P. C. Shrimpton, M. C. Hillier, M. A. Lewis and M. Dunn, "National survey of doses from ct in the uk: 2003," *Br J Radiol*, vol. 79, pp. 968-980, Dec. 2006.